

On the optical properties of Ag^{+15} ion beam irradiated TiO_2 and SnO_2 thin films

Hardeep Thakur, K. K. Sharma, and Ravi Kumar

Center for Material Science and Engineering, National Institute of Technology, Hamirpur - 177 005, India

Pardeep Thakur

*European Synchrotron Radiation Facility, BP 220, F-38043 Grenoble Cedex, France**

Abhinav Pratap Singh

Pohang Light Source, San31 Hyojadong, Namgu, Pohang -790 784, Republic of Korea

Yogesh Kumar

Material Science Division, Inter University Accelerator Centre, New Delhi 110067, India

Sanjeev Gautam and Keun Hwa Chae[†]

Nano Analysis Center, Korea Institute of Science and Technology, Seoul 136 – 791, Republic of Korea

(Dated: Received May 11, 2022)

The effects of 200 MeV Ag^{+15} ion irradiation on the optical properties of TiO_2 and SnO_2 thin films prepared by RF magnetron sputtering technique were investigated. These films were characterized by the UV-vis spectroscopy and it was observed that with increase in irradiation fluence the transmittance for the TiO_2 films systematically increases while that for SnO_2 decreases. Absorption spectra of the irradiated samples showed a minor changes in indirect bandgap from 3.44 to 3.59 eV for TiO_2 while that for SnO_2 significant modifications in the direct bandgap from 3.92 to 3.6 eV were observed on increasing irradiation fluence. The observed modifications in the optical properties of both TiO_2 and SnO_2 systems with irradiation can be attributed to controlled structural disorder/defects in the system.

PACS numbers: 78.66.Li; 68.55.-a; 78.20.Ci; 71.20.Nr

Keywords: SHI irradiation; optical properties; UV-vis; surface modifications

I. INTRODUCTION

Due to increasing interest in electronics and optoelectronics, among the wide band gap semiconductors, TiO_2 and SnO_2 are being considered as the most promising materials in view of their unique properties and various future technological applications. These applications boast their moderate price, high-volume, nontoxicity and chemical stability. In addition, these materials offer the possibility of integrating their magnetic and electronic properties in spintronic devices, which make the use of both spin and charge of the electrons [1, 2].

TiO_2 is a very interesting and versatile material with a wide range of applications, including use in microelectronics due to its high dielectric constant and in optical coatings because of its high refractive index [3–8]. It also has excellent optical transmittance in the visible and near-infrared region. TiO_2 exists in three crystalline polymorphs: rutile, anatase, and brookite with their band gap values 3.03, 3.19, and 3.11 eV respectively [9]. Among different TiO_2 polymorphs, anatase (tetragonal, D_{4h}^{19}) is a metastable phase which contains

four shared edges per octahedron (the highest condensation of TiO_6 octahedra) and is known to be useful for photocatalysis with response to ultraviolet photons. The rutile (tetragonal, D_{4h}^{14}) is thermodynamically most stable phase at all the temperatures and is formed by sharing two edges per octahedron (the lowest condensation of TiO_6 octahedra) with largest index of refraction. The brookite (orthorhombic, D_{4h}^{15}) is the most distorted phase which shares three edges per octahedron. The properties of TiO_2 are significantly dependent on the crystalline phases, i.e.; anatase, rutile, or brookite and the morphology of the material [10].

On the other hand, tin dioxide (SnO_2) has been investigated in view of potential technological applications in catalysis, gas sensor technology etc. [11–13], because of high carrier density, optical transparency, wideband gap (~ 3.6 eV), and remarkable chemical and thermal stabilities. SnO_2 exists in the most important form of crystalline phase known as cassiterite with a rutile (tetragonal, D_{4h}^{14}) structure. Another form of SnO_2 with an orthorhombic structure is known to be stable only at high pressures and temperatures.

Many deposition techniques (pulsed laser deposition, sol-gel deposition etc.) have been employed to synthesize TiO_2 and SnO_2 thin films, although magnetron sputtering remains the preferred method due to better coating uniformity, the process versatility, large area coatings and more freedom in selecting of deposition conditions[14].

*Diamond Light Source Ltd., Didcot, Oxfordshire, OX11 0DE, UK

[†]Electronic address: khchae@kist.re.kr(K.H. Chae); Phone/Fax: ++82-542791192/1599

Any mechanism that affects the lattice structure of the TiO_2 and SnO_2 systems also influences their electronic structure and optical properties. Swift heavy ion (SHI) irradiation is one of the mechanisms which have been used to tailor the material properties by modifying its electronic structure [14–16]. It is well documented that, their radiation induced defects produced in the material entirely depends upon the energy loss processes, namely; nuclear energy loss (elastic process), and electronic energy loss (inelastic process) involved during the passage of ion in the target material. In the high energy regime, due to dense electronic excitations, SHI induces point/cluster/columnar defects and structural disorder depending upon the extent of electronic energy loss mechanism in the system. The previous studies on TiO_2 and SnO_2 systems were only focused on the SHI induced modifications in the electronic structure, orbital anisotropy and magnetic properties [15, 16]. Thus, other properties, such as, optical properties, need further study.

This experimental study was conducted to observe the changes in the optical transmittance, absorption and band gaps of TiO_2 and SnO_2 thin films, irradiated with 200 MeV Ag^{+15} ion beam at various irradiation fluences ranging from 1×10^{11} to 5×10^{12} ions/cm² that deviate from what is largely reported.

II. EXPERIMENT AND DISCUSSION

The pure Titanium (II) oxide (TiO) and SnO_2 compound (purity 99.9%) were used as the starting materials for the deposition of thin films. TiO_2 and SnO_2 films, approximately ~ 100 nm thick, were deposited on cleaned sapphire single crystal substrates by using RF magnetron sputtering technique. The pure oxide materials were ground into fine powder in an agate mortar and then mixtures were pressed in the form of circular targets of 50 mm diameter by applying a pressure of 5–6 tons in a hydraulic press. The targets were sintered at 1000°C for ~ 12 hours. Prior to filling up sputtering gas the chamber was evacuated to a base pressure of $\sim 1.1 \times 10^{-5}$ Torr by the turbo molecular pump. The deposition was carried out in a partial pressure of 10 mTorr of oxygen and Ar gasses mixture (1:1) keeping the substrate temperature at 550°C and RF power 100 W. After deposition the films were annealed in-situ at 550°C in oxygen for 1 h. The deposited thin films were irradiated with 200 MeV Ag^{+15} ions to fluences of 1×10^{11} , 1×10^{12} , and 5×10^{12} ions/cm² at room temperature (RT) using the 15UD tandem accelerator at Inter University Accelerator Centre, New Delhi, India.

The structural analysis of the pristine and irradiated TiO_2 and SnO_2 films has been carried out using the high resolution x-ray diffraction (HRXRD) with $\lambda = 1.5425\text{\AA}$, at the bending magnet 10B XRS KIST-PAL beamline of the Pohang Accelerator Laboratory (PAL), S. Korea. The HRXRD profiles are shown in Fig. 1(a) for the pristine and SHI irradiated TiO_2 thin films. As shown in

Fig. 1a, the pristine sample as a tetragonal anatase structure (JCPDS, Card No.84-1286) while on irradiation at the highest SHI fluence of 5×10^{12} ions/cm², the inset in the Fig.1a clearly shows mixed peaks of the brookite (JCPDS, Card No.76-1937) and the rutile phases of TiO_2 . The appearance of broader brookite peaks clearly indicates that SHI has induced structural disorder and/or strain in the films [16]. Figure 1b shows HRXRD pattern of the pristine and SHI irradiated SnO_2 thin films collected at RT. For the pristine sample depicted in Fig. 1b, it is evident that the characteristic peaks at $2\theta = 24.20^\circ, 41.40^\circ, 41.90^\circ$ correspond to the reflections from (110), (211), and (116) planes of the orthorhombic phase (JCPDS, Card No.78-1063) of SnO_2 , respectively. The inset in the Fig. 1b shows the extended view of diffraction peaks of the pristine sample. At highest SHI fluence of 5×10^{12} ions/cm², the irradiation causes partial amorphization and/or strain in the SnO_2 system. The detailed structural verification of the SnO_2 orthorhombic structure and the effect of SHI irradiation on its structure is discussed elsewhere [17].

The optical transmittance of the pristine and irradiated thin films of both oxides were measured by collecting the transmittance spectra as a function of wavelength in the range of 200 – 800 nm at RT with a resolution of $\lambda = 0.5$ nm, using Hitachi-U3300 spectrophotometer. Figure 2 presents optical transmittance spectra for the pristine and SHI irradiated TiO_2 (upper panel) and SnO_2 (bottom panel) thin films collected at RT. It is clear from Fig.2 that the pristine TiO_2 film exhibits a transmittance value of about 25% in the visible region at ~ 470 nm. With increasing irradiation (SHI: $1 \times 10^{11} - 5 \times 10^{12}$ ions/cm²) fluence the transmittance increases considerably, which at highest fluence (SHI: 5×10^{12} ions/cm²) acquires a value of $\sim 70\%$. The increase in the transmittance with SHI fluence signifies that the transparency of SHI irradiated TiO_2 films is superior to that of the pristine film. On the other hand, the pristine SnO_2 film exhibits a systematic decrease in the transmittance with increasing irradiation (SHI: $1 \times 10^{11} - 5 \times 10^{12}$ ions/cm²) fluence. In the visible region, the transmittance for the pristine SnO_2 film was of $\sim 50\%$, which is decreased to $\sim 35\%$ for the highest SHI fluence. Moreover, at ~ 350 nm the transmittance decreases quickly for all the samples for both the oxides materials and approaches to zero at ~ 300 nm. This fast decrease in the transmittance is due to strong absorption of light in this region caused by the excitation and migration of electrons from the valence band to the conduction band. Typical oscillations in the transmittance spectra particularly for SnO_2 can be due to interference of light transmitted through the thin film and the substrate [18].

The previous studies [16, 17, 19] reveal that the irradiated TiO_2 thin films for the highest SHI fluence exhibit a mixed (dominating brookite + rutile) phase of TiO_2 while the SnO_2 pristine film is composed of a pure orthorhombic phase of SnO_2 and SHI has induced controlled structural disorder (distortion in the SnO_6 octa-

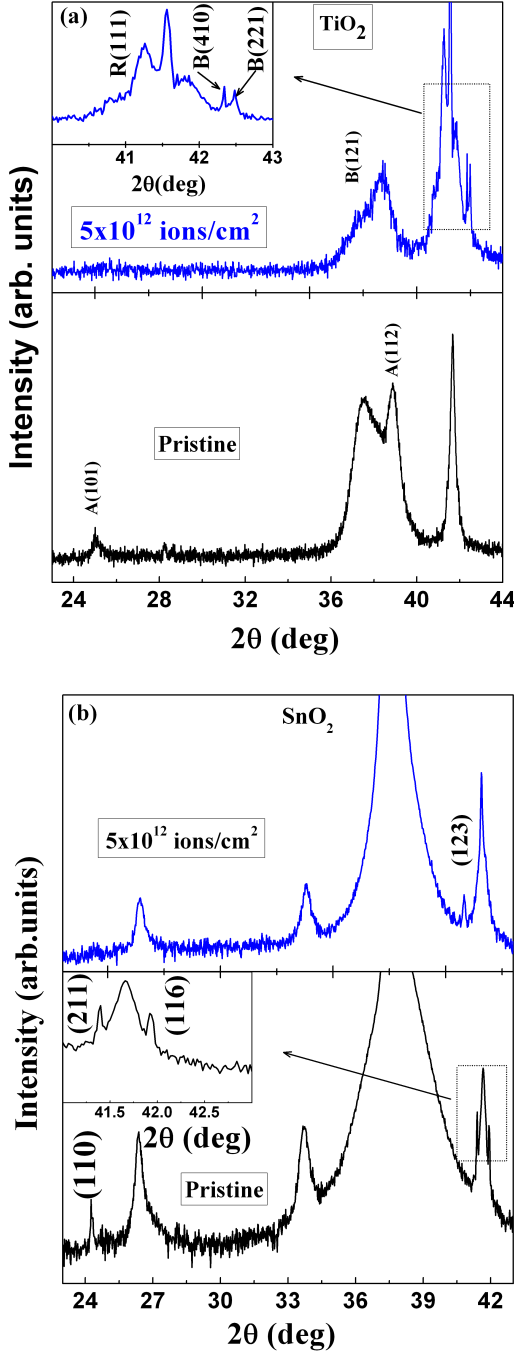


FIG. 1: HRXRD pattern of: (a) pristine and irradiated (SHI: 5×10^{12} ions/cm²) TiO₂ thin films and (b) pristine and irradiated SnO₂ thin films. The inset in Fig. 1(a): shows the extended view of the mixed brookite and rutile phases of the irradiated film and in (b): shows the extended view of the orthorhombic phase of SnO₂.

hedra) and/or strain in the films. The dominating structure of brookite phase in the SHI irradiated TiO₂ films and orthorhombic distortions of the SnO₂ lattice could have an important implication on its electronic structure and possible optical properties. Therefore, the observed changes in the transmittance of the pristine TiO₂ and

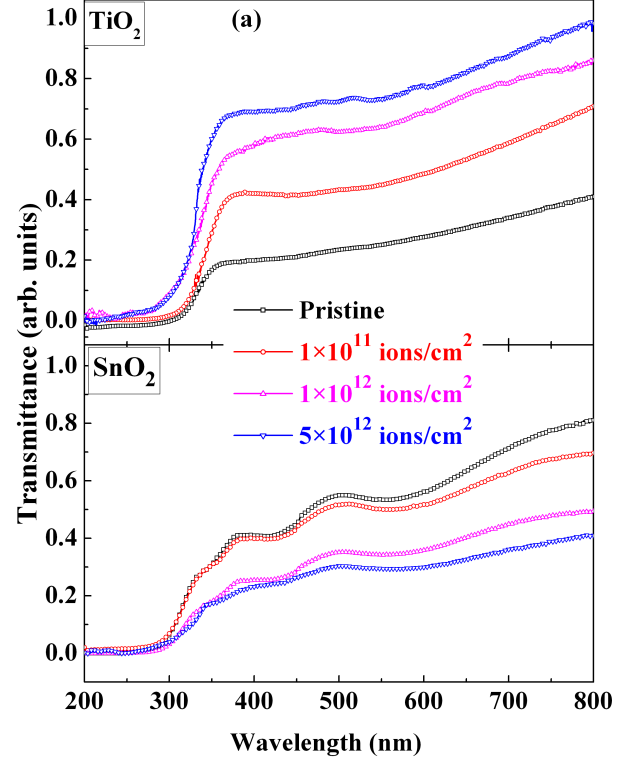


FIG. 2: Transmittance spectra for the pristine and irradiated (SHI: $1 \times 10^{11} - 5 \times 10^{12}$ ions/cm²) TiO₂ (upper panel) and the SnO₂ (bottom panel) thin films collected at RT.

SnO₂ films with SHI fluence can be attributed to TiO₆ and SnO₆ octahedral distortions respectively.

The absorption spectra for the pristine and irradiated TiO₂ and SnO₂ films were measured by collecting the absorbance as a function of wavelength at RT. The absorbance is given according to Eq.1.

$$A = \log \left(\frac{I}{I_0} \right) \quad (1)$$

where I_0 is the intensity of incident radiation and I is the transmitted intensity.

Figure 3 depicts the absorption spectra for the pristine and SHI irradiated TiO₂ (upper panel) and SnO₂ (bottom panel) thin films. The optical absorption spectra of TiO₂ showed a clear absorption edge at ~ 352 nm for the pristine TiO₂ sample. With increasing irradiation (SHI: $1 \times 10^{11} - 5 \times 10^{12}$ ions/cm²) fluence the absorption edge is slightly shifted to the smaller wavelength side and at the highest irradiation (SHI: 5×10^{12} ions/cm²) fluence it acquires a value ~ 345 nm. The observed values of the absorption edge deviate from the reported values in the literature [9]. For the SnO₂ system the optical absorption edge of the pristine film was found to be at ~ 335 nm, which is shifted to ~ 325 nm at the highest SHI fluence. In this study, an anomalous trend was observed for the optical absorption edges and the suppression in the maximum absorption with increasing SHI fluence for both the oxide materials. The absorption spectra of both

the systems reveal that the films grown under the same parametric conditions have low absorbance in the visible/near infrared region while absorbance is high in the ultraviolet region. Since SHI induces a controlled structural disorder (TiO_6 and SnO_6 octahedral distortions) in both the systems, modification in the absorption spectra can be correlated to changes in the electronic structure as a result of lowering in the orbital symmetry (i.e. its s -, p -, and d -like character) via strong hybridization effects after irradiation.

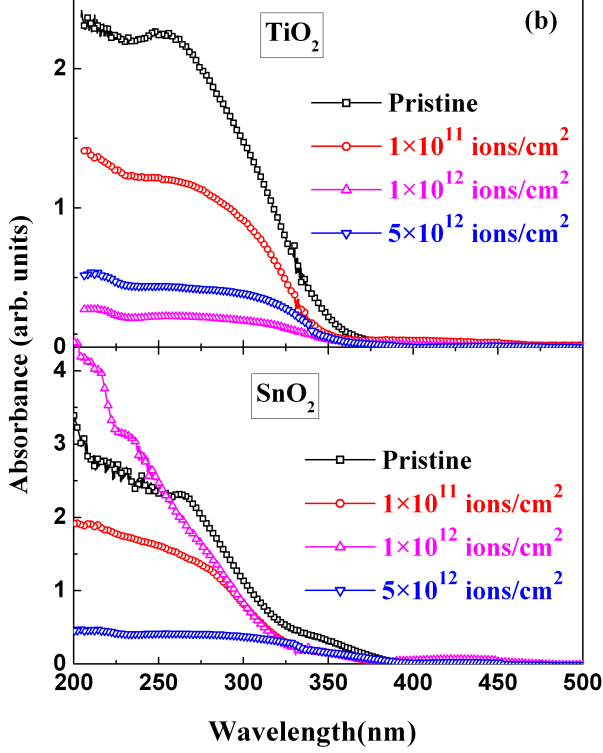


FIG. 3: Optical absorption spectra for the pristine and irradiated (SHI: $1 \times 10^{11} - 5 \times 10^{12}$ ions/ cm^2) TiO_2 (upper panel) and the SnO_2 (bottom panel) thin films collected at RT.

The variation of absorption coefficient as a function of photon energy for allowed indirect transitions [19] is given by Eq. 2,

$$\alpha = B_i(h\nu - E_g \pm E_p)^2 \quad (2)$$

and for allowed direct transitions by Eq. 3.

$$\alpha = B_d(h\nu - E_g)^{1/2} \quad (3)$$

where α is the absorption coefficient, B_i and B_d are constants for indirect and direct transitions, h is Planck's constant, ν is the frequency, E_p is the photon energy involved in the indirect transition, and E_g is the band gap energy. The absorption coefficient α is obtained from Beer's law,

$$I = I_0 \exp(-\alpha t) \quad (4)$$

In the Eq. 4, t is the thickness of the measured sample.

The relationship between the absorbance A , absorption coefficient α , and thickness of the film t is given according to Eq. 5.

$$\alpha = 2.303 \left(\frac{A}{t} \right) \quad (5)$$

A plot of $\alpha^{1/2}$ versus energy was used to obtain the value of indirect band gap and α^2 versus energy was used for the direct band gap by extrapolating the linear portion of the curves to zero absorption.

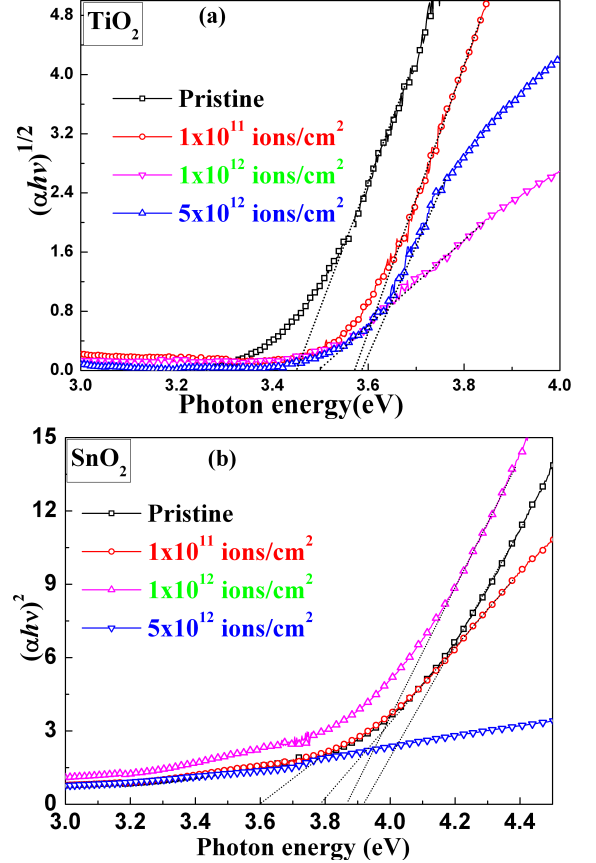


FIG. 4: Plots of: (a) $(\alpha h\nu)^{1/2}$ versus $h\nu$ for the pristine and SHI irradiated TiO_2 thin films and (b) $(\alpha h\nu)^2$ versus $h\nu$ for the pristine and SHI irradiated SnO_2 thin films collected at RT.

TABLE I: The band gap values of 100 nm thick pristine TiO_2 and SnO_2 films and irradiated by 200 MeV Ag^{+15} ion beam

Irradiation fluence (ions/ cm^2)	Band gap values	
	TiO_2	SnO_2
Pristine	3.44	3.92
1×10^{11}	3.57	3.78
1×10^{12}	3.50	3.86
5×10^{12}	3.59	3.60

The variations in the band gap for the pristine and SHI irradiated TiO_2 thin films are depicted in the Fig.4a. The

optical transitions for TiO_2 have been shown to be predominantly indirect [20, 21] while that for SnO_2 direct [22]. The overall values obtained for all the irradiation fluences are higher than the reported values for TiO_2 , usually reported around 3.2 eV. The highest band gap value was obtained for the sample irradiated at fluence 5×10^{12} ions/cm² at ~ 3.6 eV. The band gap values increased until a SHI fluence of 1×10^{12} ions/cm², where it is slightly decreased from the irradiated sample at SHI fluence of 1×10^{11} ions/cm², 3.6 – 3.5 eV. For the SnO_2 irradiated samples (see Fig. 4b) the similar trend is followed as that of TiO_2 irradiated samples. The highest value for the band gap of SnO_2 sample is for the pristine sample with a value of 3.92 eV. The values decreased until a SHI fluence of 1×10^{12} ions/cm², where the value slightly increases to 3.86 eV. For the irradiated sample with a fluence of 5×10^{12} ions/cm², the value again decreases to 3.6 eV. Table I shows the variations in the band gap energy with irradiation fluence of both the TiO_2 and SnO_2 systems. HRXRD data indicates that SHI creates controlled structural disorder in lattice of oxide materials. This can be responsible for the generation of defect levels near the conduction band, i.e., shallow energy levels, which can give rise to a transition from valence band to these levels instead of a band-to-band transition. Due to shallow levels, the band gap is effectively changed. This decrease of the band gap gives an indication of the stoichiometric deviation of the irradiated SnO_2 and increase in the oxygen vacancies in the SnO_2 lattice. A similar behaviour was also reported in a previous work [23], where the effect of In doping concentration on the optical band gap of nano- SnO_2 was investigated as a function of calcination temperature. Another possible explanation for the changes in the band gap value can be due to the fact that the density of surface states in the SnO_2 lattice induced are modified on irradiation.

It is observed that the values of optical absorption edges obtained in our experiments deviate to the known values reported in the literature [9, 24]. The obvious band gap energy changes of the both oxide systems indicate the possibility of band gap engineering in the as-deposited thin films by means of SHI irradiation. To understand the observed modifications in the optical properties it is necessary to analyze the possible implications of ion transport through the film. When 200 MeV Ag^{15+} ions pass through the oxide films, it loses its energy by collisions with nuclei (nuclear stopping power S_n) and inelastic collisions with electrons (electronic stopping power S_e). In the present case, for a TiO_2 film the value of $S_e \sim 12.96$ keV/nm and $S_n \sim 32.30$ eV/nm, while for a SnO_2 film the value of $S_e \sim 12.72$ keV/nm and $S_n \sim 36$ eV/nm as calculated by stopping and range of ions in matter software [25]. The vertical line marks 200 MeV of the incident ion energy, the energy used in the present work (see Fig. 5). From these values, it can be seen that at higher energies, the electronic energy loss dominates over nuclear energy loss and at energy of few hundreds of keV, the opposite is true. Thus, the inelastic electronic

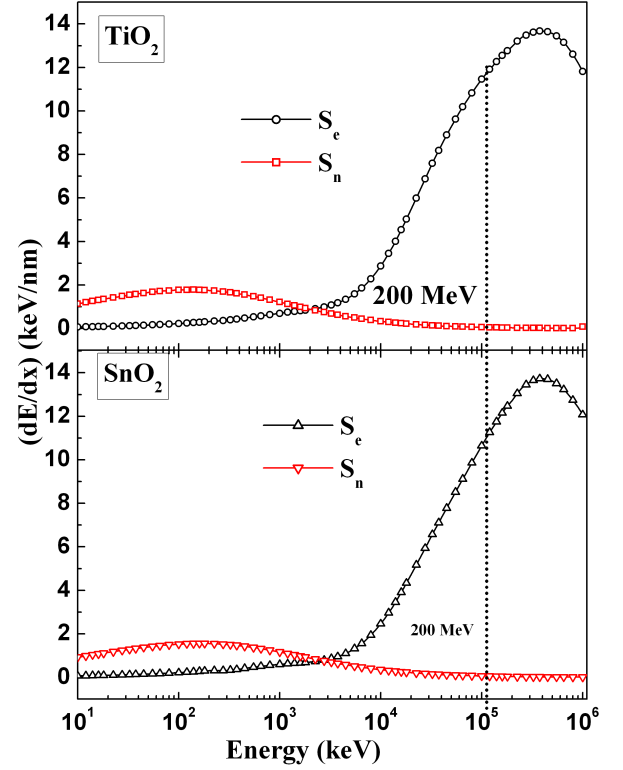


FIG. 5: The electronic and nuclear energy losses of 200 MeV Ag^{+15} ions as a function of ion energy inside TiO_2 and SnO_2 targets.

collision process is the dominant energy loss mechanism, which induces point and columnar defects and can lead to increase in defect density and modification in the lattice structure [26].

III. CONCLUSIONS

In this study, the transmittance of the TiO_2 thin films increased with increasing SHI fluence, while the transmittance of the SnO_2 thin films have been found to decrease. Both oxide systems showed improvements in the transmittance as the irradiation fluence were increased. An anomalous trend was observed for the optical absorption edges with increasing SHI fluence for both the oxide materials. For irradiated TiO_2 thin films, it has been shown that the optical band gap values for the indirect transitions are much higher than the expected values reported. The highest value of the band gap was achieved in the SHI irradiated sample at fluence 5×10^{12} ions/cm², while the lowest value of the band gap was observed in the pristine sample. Similar trend was followed in the irradiated SnO_2 samples. However, for irradiated SnO_2 thin films the band gap values on average decreased.

From the results, it can be concluded that SHI do not have critical effects on the pristine TiO_2 samples, while for SnO_2 , significant modifications in the optical properties has been observed. These observed changes in the

optical properties of the both pristine TiO_2 and SnO_2 films with SHI fluence can be attributed to controlled structural disorder/defects in the system. Our results show a direct linkage between SHI induced structural disorder/defects and the modifications in the optical properties of the oxide materials.

Acknowledgments

The authors would like to thank the Inter University Accelerator Centre, New Delhi, India and Korea Insti-

tute of Science and Technology (KIST-2V02083), Seoul 136-791, Republic of Korea for experimental supports. Department of Science and Technology (DST), Government of India, is acknowledged for supporting this work under Project No. S2/SR/CMP-0051/2007.

-
- [1] S. A. Wolf, D. D. Awschalom, R. A. Buhrman, J. M. Daughton, S. von Molánar, M. L. Roukes, A. Y. Chtchelkanova, and D. M. Treger, *Science* **294**, 1488 (2001).
 - [2] Y. Matsumoto, M. Murakami, T. Shono, T. Hasegawa, T. Fukumura, M. Kawasaki, P. Ahmet, T. Chikyow, S.-y. Koshihara, and H. Koinuma, *Science* **291**, 854 (2001).
 - [3] A. Fujishima and K. Honda, *Nature* **238**, 37 (1972).
 - [4] K. M. Glassford and J. R. Chelikowsky, *Phys. Rev. B* **46**, 1284 (1992).
 - [5] M. Ramamoorthy, R. D. King-Smith, and D. Vanderbilt, *Phys. Rev. B* **49**, 7709 (1994).
 - [6] P. J. D. Lindan, N. M. Harrison, M. J. Gillan, and J. A. White, *Phys. Rev. B* **55**, 15919 (1997).
 - [7] L. Martinu and D. Poitras, *Journal of Vacuum Science & Technology A: Vacuum, Surfaces, and Films* **18**, 2619 (2000).
 - [8] W. Brown and W. Grannemann, *Solid-State Electronics* **21**, 837 (1978).
 - [9] J.-G. Li, T. Ishigaki, and X. Sun, *J. Phys. Chem. C* **111**, 4969 (2007).
 - [10] Z. Zhang, C.-C. Wang, R. Zakaria, and J. Y. Ying, *J. Phys. Chem. B* **102**, 10871 (1998).
 - [11] M. Law, D. J. Sirbuly, J. C. Johnson, J. Goldberger, R. J. Saykally, and P. Yang, *Science* **305**, 1269 (2004).
 - [12] M. S. Arnold, P. Avouris, Z. W. Pan, and Z. L. Wang, *J. Phys. Chem. B* **107**, 659 (2003).
 - [13] Y.-S. Hea, J. C. Campbella, R. C. Murphya, M. Arendta, and J. S. Swinneaa, *J. Mater. Res.* **8**, 3131 (1993).
 - [14] H. K. and Pulker, *Surface and Coatings Technology* **112**, 250 (1999).
 - [15] D. K. Shukla, R. Kumar, S. Mollah, R. J. Choudhary, P. Thakur, S. K. Sharma, N. B. Brookes, and M. Knobel, *Phys. Rev. B* **82**, 174432 (2010).
 - [16] H. Thakur, P. Thakur, R. Kumar, N. B. Brookes, K. K. Sharma, A. P. Singh, Y. Kumar, S. Gautam, and K. H. Chae, *Appl. Phys. Lett.* **98**, 192512 (2011).
 - [17] H. Thakur, R. Kumar, P. Thakur, N. Brookes, K. Sharma, A. P. Singh, Y. Kumar, S. Gautam, and K. Chae, *Chem. Phys. Lett.* **511**, 322 (2011).
 - [18] S. Y. Kim, *Appl. Opt.* **35**, 6703 (1996).
 - [19] H. Demiryont, J. R. Sites, and K. Geib, *Appl. Opt.* **24**, 490 (1985).
 - [20] N. Daude, C. Gout, and C. Jouanin, *Phys. Rev. B* **15**, 3229 (1977).
 - [21] H. Tang, K. Prasad, R. Sanjines, P. E. Schmid, and F. Levy, *J. Appl. Phys.* **75**, 2042 (1994).
 - [22] J. Robertson, *J. Phys. C* **12**, 4767 (1979).
 - [23] C. Drake and S. Seal, *Appl. Phys. Lett.* **90**, 233117 (2007).
 - [24] K. B. Sundaram and G. K. Bhagavat, *J. Phys. D: Appl. Phys.* **14**, 921 (1981).
 - [25] J. Biersack and L. Haggmark, *Nuclear Instr. Methods B* **174**, 257 (1980).
 - [26] P. K. Kulriya, B. R. Mehta, D. K. Avasthi, D. C. Agarwal, P. Thakur, N. B. Brookes, A. K. Chawla, and R. Chandra, *Appl. Phys. Lett.* **96**, 053103 (2010).